ACS APPLIED MATERIALS & INTERFACES

Research Article

www.acsami.org

Improved Adhesion and Compliancy of Hierarchical Fibrillar Adhesives

Yasong Li,[†] Byron D. Gates,[‡] and Carlo Menon*[,†]

[†]Menrva Lab, School of Engineering Science, Simon Fraser University, 8888 University Drive, Burnaby, British Columbia V5A 1S6, Canada

[‡]Department of Chemistry and 4D LABS, Simon Fraser University, 8888 University Drive, Burnaby, British Columbia V5A 1S6, Canada

Supporting Information

ABSTRACT: The gecko relies on van der Waals forces to cling onto surfaces with a variety of topography and composition. The hierarchical fibrillar structures on their climbing feet, ranging from mesoscale to nanoscale, are hypothesized to be key elements for the animal to conquer both smooth and rough surfaces. An epoxy-based artificial hierarchical fibrillar adhesive was prepared to study the influence of the hierarchical structures on the properties of a dry adhesive. The presented experiments highlight the advantages of a hierarchical structure despite a reduction of overall density and aspect ratio of nanofibrils. In contrast to an adhesive containing only nanometer-size fibrils, the hierarchical fibrillar adhesives exhibited a higher adhesion force and better compliancy when tested on an identical substrate.

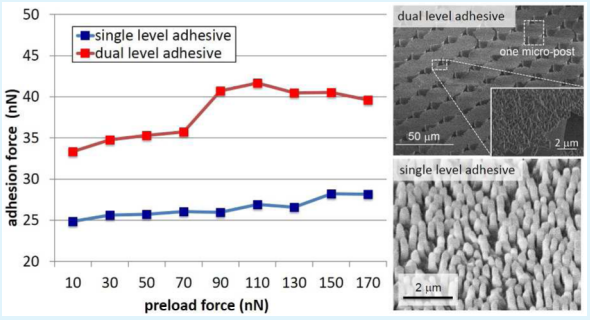

KEYWORDS: *adhesion forces, hierarchical adhesive, nanostructured fibrils, scanning probe microscopy, compliancy*

1. INTRODUCTION

The mystery of gecko's amazing ability to climb a variety of surfaces has been resolved in the past decade. This ability has been attributed to the hierarchical fibrillar structures on the gecko's feet.[1,2] These fibrils, ranging from microscale to nanoscale dimensions, are arranged within the gecko's feet in the shape of branches from a tree.[3] Millions of nanofibrils, which extend from the top surfaces of microfibrils, interact with the climbing surfaces through van der Waals forces. Numerous molecular attractive forces collectively constitute a large enough gripping force for the gecko to defy gravity. Many attempts have been made to prepare artificial fibrillar adhesives that mimic the structure of gecko's feet. In early attempts, adhesives composed by only arrays of micro- or nanofibrils were prepared using various materials and studied for their adhesion properties.[4−10] Adhesion of these adhesives can be as good as or superior to geckos' when they are tested against very flat surfaces, such as glass slides and silicon wafers. These adhesives containing only one size of fibrils have now probably reached their best possible performance, which has been achieved by reducing fibril size,[11] increasing fibril aspect ratio,[12] and changing material composition.[13]

Adhesives containing fibrils of different sizes appear to be another route to improve their adhesion performance. In an early attempt, one type of hierarchical fibrillar adhesive was prepared with a relatively simple shape that subsequently reduced the surface area of contact; adhesion performance was, therefore, worse than for a nonhierarchical structure.[14] Later, hierarchical fibrillar adhesives were prepared that had further variations in shape and size in attempts to mimic the geometry of the gecko's adhesive. Mushroom cap shape fibrils,[15] tilted fibrils with high aspect ratios,[16] reduced diameter fibrils,[17] and the used of inorganic and coating materials[18,19] were each explored as alternative methods and materials for hierarchical adhesives. Most of these researches primarily focused on studying the adhesion response of these materials and structures under an applied shear, or in other words through a measure of the frictional force.[16−18] It should, however, be noted that conditions of a high friction force typically result in irreversible fibril damage,[17,18] which is unfavorable to most applications for which dry adhesives seem to be the most suitable, such as pick-and-place automation,[16] microchip handling,[20] and design of climbing robots.[21,22] In one type of hierarchical adhesive, a demonstrated advantage of having hierarchical structures is the ability to adapt to an increased surface roughness of the test substrate.[16] On the basis of the size of the fibrils, this increase in friction might indicate that the nanofibrils induce mechanical interlocking on the rougher surfaces in addition to an increased van der Waals interaction. Another type of hierarchical adhesive, which were characterized for their pull-off force instead of their frictional force, did not yet show any improvement when compared to adhesives that

Received: April 24, 2015
Accepted: July 13, 2015
Published: July 13, 2015

ACS Publications © 2015 American Chemical Society

DOI: 10.1021/acsami.5b03576
ACS Appl. Mater. Interfaces 2015, 7, 16410−16417

only contain nanofibrils.[23] Some other hierarchical dry adhesives, which contain larger fibrils that are sandwiched by thin sheets of polymer, are not suitable for a direct comparison to those hierarchical structures having separate microfibrils since they have a radically different geometry.[24−26]

Two previously reported studies are particularly relevant to the work presented here with implications to both the preparation and testing of gecko-inspired adhesives. Mohrig et al. used a three-dimensional (3D) laser photolithography method to prepare hierarchical fibrils with control over their aspect ratio, cap shape, density and tilt angle with respect to the substrate.[27] The adhesion force of these fibrils was measured using an atomic force microscope (AFM) and a colloidal probe, which combines a flat cantilever with an attached borosilicate sphere that was brought into contact with the array of fibrils. The sphere diameter (~20 μm) was much larger than the diameter of both the nanofibrils and microfibrils. The use of the AFM enabled a correlation between adhesion forces and the physical topography of the hierarchical structures. The adhesion force and topography were represented in two-dimensional plots, which were referred to as adhesion force map and height map. Correlations between the two maps could be determined by matching pixels located at the same coordinate in the adhesion force and height maps. Although the conclusion of this study was that their hierarchical fibrillar adhesive did not demonstrate an improvement of the adhesion properties over those for nanofibrillar adhesives,[27] the massive amount of data acquired on the adhesion response with changing preload provided further insight into the properties of the adhesive. Large standard deviation in the measured adhesion for the hierarchical structure indicated the structure introduce more uncertainty than in the measurements for a single level adhesive. The mushroom cap structure did, however, show a positive effect on the adhesion.

In a second study that is also very relevant to our own studies, Lee et al. used a soft material to demonstrate an enhancement of adhesion in hierarchical fibrillar adhesives.[28] The shape of the fibrils in their hierarchical adhesives was much closer to that in a gecko adhesive than those analyzed in the study described above.[27] Using an AFM with a colloidal probe, the measured adhesion force of the soft hierarchical adhesive was twice as high as that for a single level fibrillar adhesive with an aspect ratio of 5:1, length/diameter. Analysis of the frictional force response versus preloading force was performed in this study, but the results were not relevant to structure compliancy.

These previous studies also demonstrated a few limitations. First, the preparation of hierarchical fibrillar adhesives was generally expensive because of the required instrumentation or customized materials. Second, most of these studies demonstrated no improvement on the pull-up force in comparison to that for single level adhesives. Third, very few studies investigated normal adhesion. Finally, characterization methods provided limited information on compliancy enhancement from the hierarchical structure.

In this Research Article, a low cost and high yield method to prepare hierarchical fibrillar adhesives is introduced and characterized. Importantly, this hierarchical adhesive demonstrated enhanced normal adhesion forces comparing to the adhesive only containing nanofibrils. Correlation between structural compliancy and adhesion enhancement is discussed. The successful fabrication of such hierarchical adhesive can potentially find use in applications requiring large scale reusable adhesives, such as pick and place tools[16] and climbing robots.[21,22,37]

2. SAMPLE PREPARATION AND EVALUATION METHOD

2.1. Preparation of Hierarchical Fibrillar Arrays. The hierarchical fibrillar arrays were prepared using epoxy (TC-1622, BJB enterprise). An overview of the procedures used in the preparation of the hierarchical fibrillar arrays is illustrated in Figure 1. First, microscale fibrillar arrays were fabricated using photo-

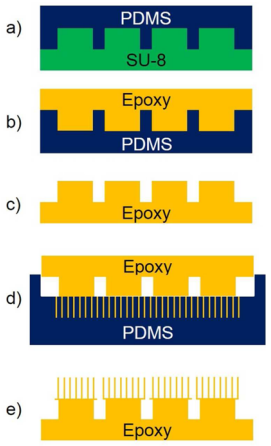

Figure 1. Schematic procedure for the preparation of the hierarchical nanostructured adhesives. (a) A liquid PDMS precursor was poured over arrays of circular micrometer-size pillars, which were fabricated from SU-8 using photolithographic techniques; (b) a liquid epoxy precursor was poured into the circular micrometer-size holes in the PDMS mold prepared following demolding in the previous step; (c) the epoxy was cured and separated from the PDMS mold; (d) the arrays of epoxy micropillars were brought into contact with a PDMS mold containing arrays of nanoholes prefilled with a liquid epoxy; and (e) epoxy in the arrays of nanoholes was cured and the entire piece of epoxy peeled from the PDMS mold. Schematics are meant for representation of fabrication procedures only.

lithography. Circular microfibrils with a diameter of ~10 μm were fabricated using SU-8 (diluted from SU-8 2050, solid contents 58%, MicroChem) on a polished silicon wafer substrate. The microfibrils were arranged in arrays upon the silicon wafer. Spaces in between the microfibrils were 5 μm, and the microfibrils were ~20 μm in height. Selection of microfibril geometry was based on the result of a previous work on optimizing polymeric microfibrillar adhesives.[29] The microfibrils supported on a silicon wafer were subsequently placed into a desiccator for coating with a release layer. A scintillation vial cap containing 30 μL of a mold release agent (1*H*,1*H*,2*H*,2*H*-perfluorodecyldimethylchlorosilane, Alfa Aesar, >90%) was placed beside the silicon wafer overnight in the desiccator while vacuum was applied to the chamber. The wafer was subsequently examined for its hydrophobicity by measuring static water contact angles. The silicon wafer originally had a static water contact angle of ~20 degrees. The static water contact angle increased to ~90 deg after deposition of the silane coating. The silane coated microfibrils and silicon wafer were immersed in a precursor to polydimethylsiloxane (PDMS, Sylgard 184, Dow Corning) as depicted in Figure 1a. The PDMS negative mold containing arrays of microholes was separated from the SU-8 microfibrils after completely curing the polymer for 24 h at room temperature. An epoxy precursor was mixed from its two components and poured onto the PDMS negative mold with an excess amount of epoxy precursor to form the substrate that would connect all of the microfibrils (Figure 1b). To improve the filling of the recesses within the mold, the PDMS mold with liquid epoxy precursor applied to its surfaces were placed in a vacuum chamber for 20 min to remove gases

DOI: 10.1021/acsami.5b03576
ACS Appl. Mater. Interfaces 2015, 7, 16410−16417

trapped in these recesses. The array of epoxy based microfibrils were cured over 24 h at room temperature and removed from the PDMS mold as a single piece (connected to a single substrate of cured epoxy) for further attachment of arrays of nanopillars (Figure 1c).

Preparation of arrays of nanoholes in PDMS was introduced in a previous paper,[32] which enabled a broader material choice for preparing arrays of nanofibrillar structures using arrays of nanoholes in PDMS. To attach the epoxy-based nanofibrils onto the ends of the microfibrils, freshly mixed epoxy precursor was poured on top of the array of nanoholes in PDMS, and excess liquid precursor was removed from these surfaces. The previously prepared piece of epoxy containing the arrays of microfibrils was immediately placed on top of these arrays of nanoholes, with the ends of each of the microfibrils in contact with the uncured interface of epoxy precursor within the arrays of nanoholes (Figure 1d). This stack of epoxy precursor and PDMS mold were sandwiched by two 1 mm thick glass slides and held in place using binder clips. The entire assembly was placed upon a flat surface to cure the epoxy over 24 h at room temperature. The hierarchical fibrillar structure of epoxy (Figure 1e) was removed from the PDMS mold containing the arrays of nanoholes. Scanning electron microscopes (SEM, Explorer and Helios, FEI) were used to examine the appearance of these hierarchical structures. The nanofibrils were ~200 nm in diameter and ~0.8 μm in height. A higher magnification SEM image can be found in the Supporting Information for dimension estimation of the nanofibrils.

2.2. Evaluation of Adhesion Properties in Hierarchical Fibrillar Adhesives. The adhesion force and uniformity of the hierarchical structure was examined using an atomic force microscope (AFM, MFP-3D-SA, Asylum Research) with a customized script written (with assistance from Jason Bemis, Asylum Research, Santa Barbara, CA) for moving the AFM probe in specific directions. AFM cantilevers without sharp tips (specifically cantilever "A" in HQ: NSC36/TIPLESS/CR-AU, MIKROMASCH) were used in the measurements. The cantilever was 110 μm long and 32.5 μm wide and its end had a triangular shape whose height was 18 μm (see Supporting Information document). The spring constant of the cantilever was calibrated every time the cantilever was loaded into the AFM system for a new set of measurements. The spring constant of cantilever "A" was ~1.7 N/m. There were two types of movements that the cantilever used to locate the area of interest and to measure the adhesion forces between the two contacting materials. The first type of cantilever movement is called a push−pull (PP) method, which lowers (or pushes) the cantilever vertically toward the surfaces of an adhesive until reaching a certain preload force, and subsequently the cantilever is vertically pulled up from these surfaces until the cantilever is completely separated from the fibrillar surfaces. The second type of cantilever movement is called the load−drag−pull (LDP) method, which has an extra movement in between the "push" and "pull" movements of the cantilever. The additional movement in this method consists of a horizontal displacement of the cantilever with respect to the array of fibrillar structures. The differences between these two types of cantilever movements are described in further detail in our previous work.[30−32] In this article, the PP method was used to locate the area of interest and the LDP method was used to measure the adhesion forces of the fibrillar arrays. The preload force was set to 100 nN. The contact area between the flat cantilever and the fibrillar sample is estimated to be ~0.401 μm^2. Estimation of the contact area is detailed in the Supporting Information document.

A force map and height map were obtained using the automatic script running with the AFM. The force map correlated the planar location in both X and Y directions. For example, measuring an area of 20 × 20 μm^2 with 400 individual measurements were executed using the following procedures: the AFM cantilever first finished one measurement, moved 1 μm in the X-direction (horizontal direction in the force map; moving from left to right) and performed another measurement. These procedures were repeated 20 times in the X-direction, which constructed one row of the force map. The cantilever subsequently moved 1 μm in the Y-direction (vertical direction in the force map) and continued the measurements for another row data points comprising the force map. Therefore, in each force map 400 individual measurements were performed, which were represented in a gray scale map as an array of 20 × 20 small squares. The height map represented the distance the cantilever moved toward the substrate, instead of the adhesion force in the force map, during each measurement to maintain the same preload force. The adhesion force and height information were simultaneously recorded in each measurement.

2.3. Statistical Analysis of Experimental Results. Since 400 individual measurements were acquired for each sample, a statistical analysis was required to evaluate the adhesion properties of the hierarchical structure. Histograms of the measurements on different samples were plotted to better visualize trends in the main population and its distribution. Mean values were calculated as a further indicator of the trends in the main population. Friedman test, a nonparametric ANOVA method specifically for data of non-Gaussian distribution, was performed to detect differences between the series of data collected for each experiment.

3. RESULTS AND DISCUSSION

Preparation of samples investigated in this work made use of a molding technique reported in our previous work,[32] which enabled the selection of different materials for preparing arrays of nanopillars. This method was extended to the fabrication of micrometer-size arrays of fibrils for the formation of a hierarchical fibrillar structure. Combination of the two levels of fibrillar arrays was achieved by adapting the dip and transfer method reported in the literature.[15,33,34] Advantage of using the dip and transfer method is that the excess liquid polymer can form a thin film in the shape of a mushroom cap at the interface between the scale levels of structures. Figure 2a depicts the

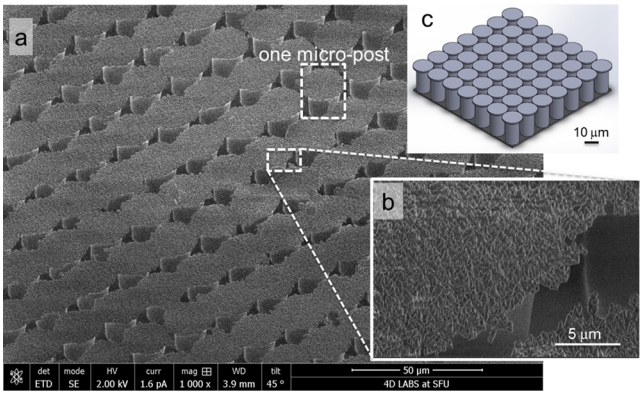

Figure 2. Hierarchical fibrillar structure examined using scanning electron microscopy (SEM) and the arrays of microposts examined using optical microscopy. (a) Arrays of hierarchical epoxy fibrils with a mushroom cap like thin film of nanofibrils supported on the ends of each micropost. (b) Magnified SEM image corresponding to the dashed box annotated in panel a. (c) Schematics of the arrays of hierarchical microfibrils, with dimension noted. Both panels a and b were obtained by SEM at a 45° stage tilt.

mushroom shape of the micrometer-size fibrils arranged in an array upon a substrate. The transferred thin film, which has a diameter slightly larger than the supporting fibril, contains arrays of low aspect ratio nanofibrils. Figure 2b shows a magnified view of this thin film. Both SEM images were taken at a 45-degree stage tilt, which enables the observation of the microfibril underneath the thin film cap. Figure 2c is a schematic of a 3D representation of the fibrillar adhesives. The close packing fibrils have their rim of the mushroom caps touching with each other. From examination of the spaces between the microfibrils, it was determined that the radius of

DOI: 10.1021/acsami.5b03576
ACS Appl. Mater. Interfaces 2015, 7, 16410−16417

the mushroom shape thin film was ~2 μm wider than the supporting fibril. Instead of dipping the arrays of microfibrils into freshly prepared precursor to the epoxy by the dip and transfer method, epoxy was poured onto the PDMS mold containing arrays of nanoholes and the excess amount of epoxy was scraped off from the mold. This scraping step created a very thin film of excess epoxy, which enabled the microfibrils to remain separate in the final hierarchical structure. This thin film of mushroom cap decreased the empty spaces due to the design of individual microfibrils, which intended to provide extra flexibility and compliancy of the entire structure. The mushroom cap itself is thin and flexible, being able to withstand and comply with compression preloads, and stretch to provide extra energy for detaching the fibrillar adhesive and the contact surfaces. Although the observable area containing nanofibrils was reduced due to the vacancies in between each microfibril, the thin film or mushroom cap shaped array of microfibrils provided improved flexibility and compliancy toward the contacting surfaces. The spaces in between the microfibrils provided enough room to sufficiently comply with rough surfaces and potentially to improve the adhesion performance of the dry adhesive. Neighboring microfibrils are seen to be connected by the excess epoxy thin layer. This thin layer is expected to confine the lateral movement of the microfibrils, but not as severe as unmovable. Instead, this close packed arrangement of microfibrils provide support for the entire structure to resist high compression preloads without damaging individual microfibrils. A detail discussion about the flexibility of the microfibrils, which proved to have enhanced compliancy toward different compression preloads, is presented in subsequent paragraph.

To assess the adhesion properties of the hierarchical fibrillar structure, we adapted a technique[30,31] that used an atomic force microscope to characterize surface uniformity and correlate physical locations in the sample with the measured adhesion force between the sample and a flat silicon nitride cantilever. Figure 3 depicts a typical set of measurements obtained from the hierarchical fibrillar structures using the PP method. These measurements covered an area of 40 × 40 μm^2, comprising of 20 × 20 independent data points (represented in Figure 3a). Both Figure 3b and c represent measurements over the same area of the sample, but report complementary information. Figure 3b represents the vertical distance traveled by the cantilever before reaching the set value for the preload force, which was 100 nN in this set of measurements. This figure provides information on the sample topography. The slightly brighter region of the upper left corner of the image indicates the substrate of the hierarchical array of fibrils was not parallel to the cantilever within the scanning head of the AFM. It is clearly observed from the height map (Figure 3b) that the data depicts 3 bright circles (numbered as circle 2, 3 and 5), each of which represents a full cap of microfibril, and several other partial circles also appear in this measured region. However, the corresponding adhesion map does not have as distinct a pattern (Figure 3c). The colored circle and oval noted on both images represent the empty regions between adjacent microfibrils. Specifically, the red solid circle indicates a region where the side of the cantilever was in contact to the edge of a post during the measurements. We believe that in this region of the sample the tip of the cantilever traveled below the surface of the thin film, referring to high depth value represented as almost black data points in Figure 3b, into the space between the mushroom caps. When the preload reached 100 nN, the cantilever was

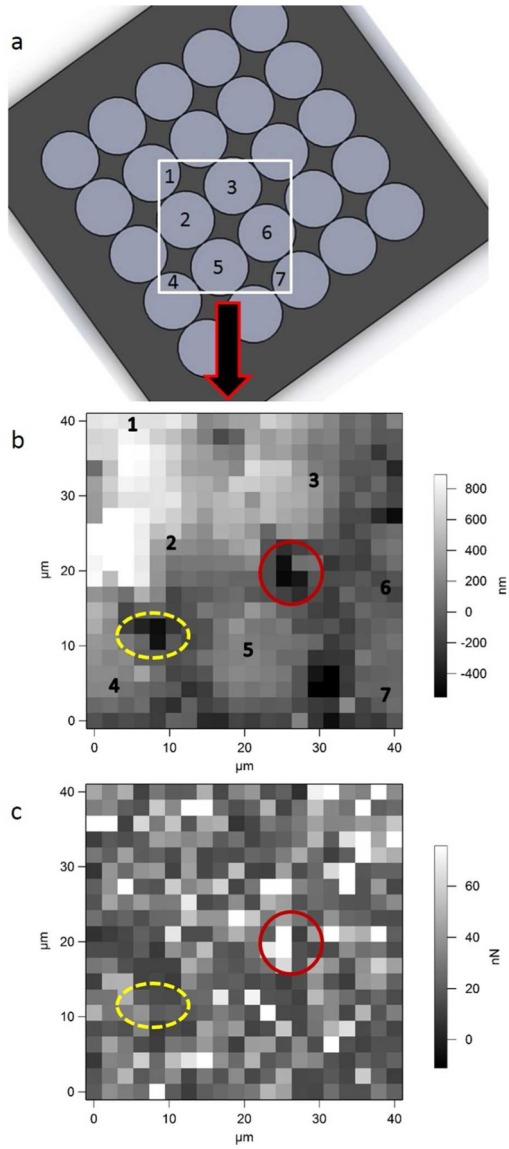

Figure 3. Correlations between height and adhesion force maps. Both sets of data (b and c) were obtained simultaneously during these measurements. (a) Schematics showing the top view of the arrays of microfibrils. The white square depicts the area being measured, which represented in the height map (b) and the adhesion map (c). (b) Height map for an array of hierarchical fibrillar adhesives, representing the 3D geometry of the measured area. (c) Adhesion force map for the same region depicted in the topography map.

underneath the thin film and got "stuck" when a pulling force was applied to the cantilever. This behavior could explain the relatively high adhesion observed (Figure 3c) in the location of the red circle. The adhesion force measured in this location was, therefore, the force required to bend the mushroom caps upward, such that the cantilever was released from these structures in the sample.

The yellow dashed ovals in Figure 3b and c depict another gap between the mushrooms caps. In this case, we believe that the thin film of the mushroom caps that surrounded the gap was thicker and the displacement of the cantilever was not sufficient to penetrate under this region of the mushroom cap. Interlocking of the mushroom cap and the cantilever was, therefore, not dominating in this case, as observed in the force map (Figure 3c).

DOI: 10.1021/acsami.5b03576
ACS Appl. Mater. Interfaces 2015, 7, 16410−16417

It should be noted that the measured force observed in the force map was randomly distributed for the hierarchical arrays when tested under the same preload conditions. The apparent disadvantage of empty regions between the separated microfibrils, which supposed to provide zero adhesion force, had a negligible effect on the observed adhesion forces. This result would be particularly important for the situation that the adhesive must comply with rough surfaces, simulated by the normal movements and small dimensions of the cantilever, where interlocking of the two surfaces may occur. These interlocking forces observed in Figure 3 are usually counted as adhesion forces in macroscopic tests.[4−7,9−15] The techniques used in our adhesion tests provide this extra information correlated to the complicated topography of the hierarchical fibrillar structure. To investigate the adhesion provided only by the fibrillar structure, adhesion measurements have been done on the area containing only the nanofibrils on different microfibrils (see Figure 4).

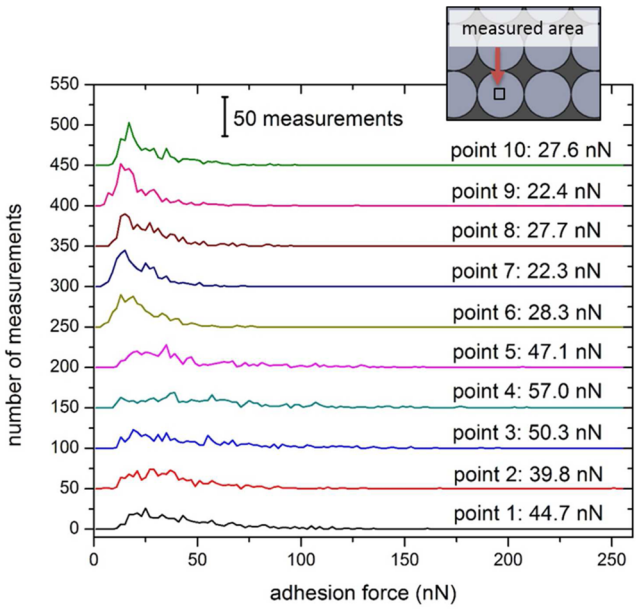

Figure 4. Line graphs of measurements obtained from 10 different micropillars. The black square in the inset showed the measured areas ($5 \times 5\ \mu m^2$) on top of the mushroom-cap. Each analysis contains 400 measurements, and these trend lines are vertically stacked with an offset of 50 measurements. Annotation above each line indicates the average value of each set of 400 measurements.

The average adhesion force for the hierarchical structures in Figure 3c was ~32 nN, which was higher than the measured average adhesion force (23.2 nN) of a single layer containing only nanofibrils.[32] To further investigate adhesion strength and uniformity, measurements were also obtained from a small area located on top of a mushroom cap (see inset of Figure 4). Measurements using the LDP method were repeated on 10 different, randomly chosen microfibrils. The results are plotted in Figure 4 with a vertical offset in the *y*-axis, which represents the total number of measured counts at each force. Each line corresponds to 400 measurements obtained from a force map over a $5 \times 5\ \mu m^2$ area corresponding to a single mushroom cap. For each of the 10 separate sets of measurements, the corresponding average adhesion force is noted on the right-hand side of each line graph (Figure 4). The average force from the total of 4000 independent measurements was 36.7 nN. The minimum and maximum average adhesion forces were 22.3 and 57 nN, respectively. This large variation in the adhesion force suggests a relatively poor uniformity of the hierarchical fibrillar adhesive. The lowest measured value (22.3 nN) was, however, similar to the average adhesion force measured using a single layer of nanofibrils (23.2 nN reported in our previous work[32]), thus indicating the overall improved performance of the hierarchical structure.

In Figure 4, these sets of measurements can be grouped into two types: either (1) relatively low or (2) high average adhesion forces. Measurements with average adhesion forces less than 30 nN are plotted in the topmost 5 line graphs (marked as points 6 to 10 in the sample). Each of these lines shows a clear peak in their overall counts. The range of measured adhesion forces in these samples is relatively small, typically within 100 nN. For measurements with an average adhesion force greater than 30 nN the corresponding line graphs are plotted in the bottom-most traces in Figure 4 (marked as points 1−5 in the sample). There was no obvious peak force in the measured counts for these five data sets; the peak was not as sharp as those observed in the other line graphs for points 6 to 10. The range of adhesion forces measured for points 1 to 5 were also much broader with a spread of up to 200 nN. In summary, the hierarchical arrays of fibrils, which overall have a higher average adhesion force than the single layers of fibrils, have broader distribution or more variation in their adhesion performance. The nonuniformity of the handcrafted scraping method to remove excess liquid epoxy precursor from the mold might be the reason for this observed phenomenon. The scraping method, which used a flat spatula, might in fact be squeezing epoxy out of some regions of the mold if the relative scrapping pressure is too high. The pressure of the spatula varies since the procedure was performed manually. Furthermore, the binder clips could provide an uneven pressure during the process that combines the epoxy micro- and nanofibrils into a single hierarchical structure, although the nonuniformities in applied pressure will be partially compensated by the backing glass slides. Variations in the conditions across the molded sample resulting from the preparation method could lead to a nonuniform performance of the hierarchical fibrillar adhesive. Despite the nonuniformity of the hierarchical fibrillar adhesive, the average adhesion forces of these structures outperformed those of the single level fibrillar adhesive. It should be noted that the nanofibrils of the single level fibrillar adhesive reported in our previous work[32] had a higher aspect ratio and a more well-defined shape than the nanofibrils within the hierarchical fibrillar adhesive presented herein. The observed improvement in adhesion of the hierarchical fibrillar adhesive is attributed solely to the changes in geometry of the fibrils, since the material composition was identical between these two types of samples.

To further investigate the effect of geometry on the fibrillar adhesive, measurements on a freshly prepared single level nanostructured adhesive were compared with those from the hierarchical fibrillar adhesive. A range of different preloading forces was investigated to reveal the compliancy of these structures. The single level nanostructured adhesive contained the similar topography as reported in our previous work.[32] Measurements performed in this comparative study were obtained using the LDP method. From this point forward in the discussion, the *single level adhesive* refers to adhesive that is comprised of arrays of only nanofibrils; the *dual level adhesive* refers to the hierarchical fibrillar adhesive that contained arrays

DOI: 10.1021/acsami.5b03576
ACS Appl. Mater. Interfaces 2015, 7, 16410−16417

of both microfibrils and nanofibrils. Figure 5 illustrates the effect of varying the preload force on the measured adhesion

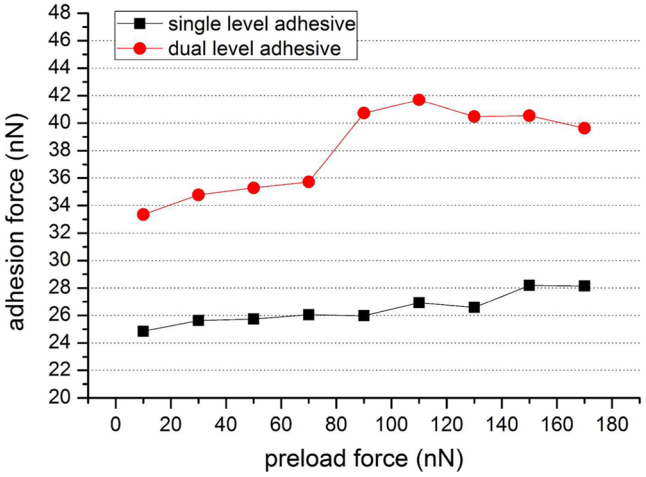

Figure 5. Average adhesion forces measured for samples containing either nanofibrils or hierarchical fibrillar structures as a function of different applied preload forces. Every data point in the graph, either for the single layer adhesive (only containing the nanofibrils) or the dual level adhesive (containing both micrometer-size and nanometer-size fibrils), was measured over the same area while changing the preloading force.

forces for both the single and dual level adhesives. The measured area was held unmoved for each sample. Each data point is the average adhesion force from 400 independent measurements obtained from a single force map. Adhesion forces increased in proportion to the increase in preloading force for both the single and dual level adhesives. The rate of observed increase in adhesion force for the dual level adhesive is more than two times greater than that for the single level adhesive, if using a linear trend line to estimate the increasing rate. Adhesion force differences between the single level adhesive and the dual level adhesive were also investigated using a statistical method. Suspecting that the data were not from normal distributed populations, the Friedman test, a nonparametric statistical test, was performed on the two series of data. The p-value of this test was much smaller than 0.01, which indicated there were substantial differences in adhesion forces between the two samples. The slight decrease in adhesion force for the hierarchical structure at a preloading force of 170 nN raised concerns for fibril damage and adhesion force saturation. Measurements were, therefore, performed using a preloading force of 300 nN to further investigate the possibility of either scenario. The 300 nN preloading force was selected because of the maximum deformation this particular cantilever could withstand. Average adhesion forces measured, using a 300 nN preload force, were 31.2 nN on the single level adhesive and 42.3 nN on the dual level adhesive. The enhanced adhesion force measured using a higher preloading force suggested a limited damage to the fibrils, which was further confirmed by SEM analysis of the tested regions of the samples. The high variation observed in the data points for the dual level adhesive (Figure 5) is, therefore, attributed to deformation of the microfibrils. Specifically, during adhesion force measurements using the LDP method, the shear movement applied to the sample could cause the microfibrils to bend rather than sliding over the nanofibrils with the AFM cantilever. After overcoming the microfibril deformation with a higher compression force, nanofibrils were severely bent and adjust themselves to conform to a less stressed position. We believe that the tips of the fibrils overcome the initial static friction and release the stress of deformation while the flat cantilever continues compressing them (please see the cantilever deflection curves in the Supporting Information, which depict the cantilever response during dragging for preloading forces of 10 nN and 70 nN). Once the compression force passes a threshold that causes the deformation of fibrils, which was represented by the observed plateau in the measurements between 10 and 70 nN (Figure 5), the advantage of having microfibrils becomes more relevant. This advantage is observed in the subsequent increase in measured adhesion force associated with the large increase in the adhesion force measured when changing from a preload force of 70 nN to 90 nN. The flexibility provided by the arrays of microfibrils enhances the process of aligning the nanofibrils, which subsequently increases the measured adhesion force (see Supporting Information document).

Histograms of the vertical displacement of the AFM tip for both single and dual level adhesives are plotted in Figure 6.

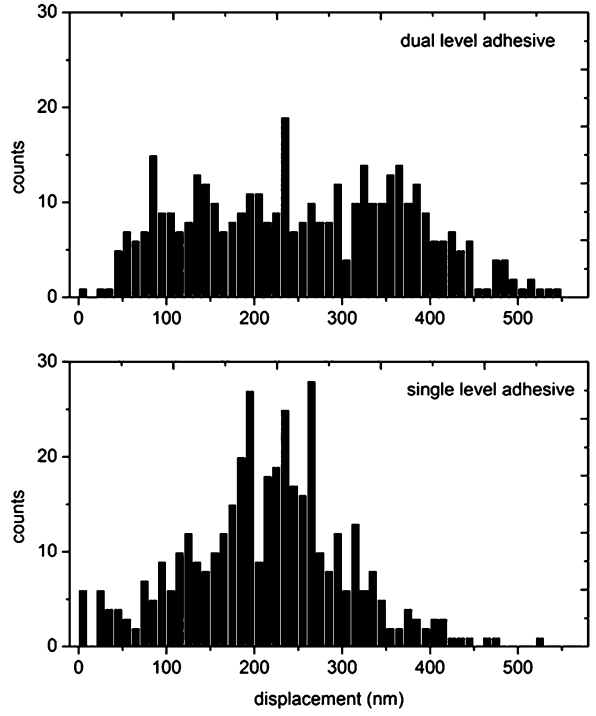

Figure 6. Histograms of the vertical deformation measurements on dual and single level adhesives. The preloading force reached 100 nN for each of the 400 measurements that were performed.

Each histogram consists of independent measurements obtained by first placing the AFM cantilever in contact with the sample and then gradually increasing its preloading force up to a maximum of 100 nN. The vertical displacement when this preload was applied was recorded in 400 locations distributed in the sample.

Two primary conclusions can be drawn from the two histograms of Figure 6. The first conclusion is that the hierarchical adhesive was more compliant than the single level adhesive. In fact, the median of vertical displacement for the dual and single level adhesives was, respectively, 250 and 217

DOI: 10.1021/acsami.5b03576
ACS Appl. Mater. Interfaces 2015, 7, 16410−16417

nm. The enhanced compliancy supports the hypothesis that adhesion forces increased through the use of a hierarchical fibrillar structure.

The second conclusion is that the variability of the dual level adhesive in terms of vertical deformation was higher. In fact, while the histogram of the single level adhesive presents a distribution that is close to a Gaussian distribution and has a well-defined peak (Kurtosis 0.2), the histogram of the dual level adhesive is much more evenly distributed (Kurtosis −0.9). This observation is also confirmed by the variance of these two histograms - the variance observed in the dual level adhesive is 1.5×10^4 nm^2, which is almost two times higher than the one of the single level adhesive (0.84×10^4 nm^2). The high variance and the negative Kurtosis of the histogram of the dual level adhesive imply it has a flat distribution.[35] The flatter distribution of the hierarchical adhesive indicates that the variability of its stiffness was higher than the one of the single layer adhesive. This result was expected, as the stiffness at the center of each micropost is higher than at the edge of its mushroom cap.[27] This variability in compliancy is believed to facilitate adhesion to surfaces with high topographic variability. This aspect is however to be verified in future studies needed to extensively and methodologically test the adhesive behavior against a large number of surfaces having different values of roughness.

4. CONCLUSION

This work presented a hierarchical fibrillar adhesive prepared using epoxy. The hierarchical adhesive comprised of two levels of fibrils in both micro- and nanometer size. The "dip and transfer" method yielded mushroom shape microfibrils. A measurement technique was implemented using an atomic force microscope to characterize the adhesion properties of the hierarchical structures. The average adhesion force of the hierarchical fibrillar adhesive was generally greater than that measured for an adhesive only containing a single level of nanofibrils. Given that the material composition of both the single and dual level adhesives was identical, these results suggest that the improvement in measured adhesion force was because of the hierarchical structure of the dual level, which provided higher compliancy. Hierarchical fibrillar adhesives could find a large range of applications and enable new products to be developed such as equipment for handling liquid-crystal-displays,[16] skin patches for medical use,[36] and wall climbing robots.[37]

■ ASSOCIATED CONTENT

Supporting Information

Estimation of the contact area between the arrays of fibrils and the flat cantilever during force measurement, SEM images of a close up view of the nanofibrils on the hierarchical fibrillar structure, and discussion on the possible mechanisms responsible for the behavior recorded during LDP measurements are described in the Supporting Information. The Supporting Information is available free of charge on the ACS Publications website at DOI: 10.1021/acsami.5b03576.

■ AUTHOR INFORMATION

Corresponding Author

*E-mail: cmenon@sfu.ca.

Notes

The authors declare no competing financial interest.

■ ACKNOWLEDGMENTS

This work was supported in part by the Natural Sciences and Engineering Research Council (NSERC) of Canada, and the Canada Research Chairs Program (B.D. Gates). This work made use of 4D LABS shared facilities supported by the Canada Foundation for Innovation (CFI), British Columbia Knowledge Development Fund (BCKDF), Western Economic Diversification Canada, and Simon Fraser University. We appreciate the assistance of Jason Bemis at Asylum Research for assistance in codeveloping the software necessary for measuring adhesion forces resulting from shear induced alignment of fibrils using scanning probe microscopy techniques.

■ REFERENCES

(1) Autumn, K.; Liang, Y.; Hsieh, T.; Zesch, W.; Chan, W.-P.; Kenny, T.; Fearing, R.; Full, R. J. Adhesive Force of a Single Gecko Foot-Hair. *Nature* **2000**, *405*, 681−685.

(2) Autumn, K.; Sitti, M.; Liang, Y. A.; Peattie, A. M.; Hansen, W. R.; Sponberg, S.; Kenny, T.; Fearing, R.; Israelachvili, J. N.; Full, R. J. Evidence for van der Waals Adhesion in Gecko Setae. *Proc. Natl. Acad. Sci. U. S. A.* **2002**, *99*, 12252−12256.

(3) Autumn, K. Gecko Adhesion: Structure, Function, and Applications. *MRS Bull.* **2007**, *32*, 473−478.

(4) Geim, A. K.; Dubonos, S. V.; Grigorieva, I. V.; Novoselov, K. S.; Zhukov, A. A.; Shapoval, S. Y. Microfabricated Adhesive Mimicking Gecko Foot-Hair. *Nat. Mater.* **2003**, *2*, 461−463.

(5) Glassmaker, N. J.; Jagota, A.; Hui, C.-Y.; Kim, J. Design of Biomimetic Fibrillar Interfaces: 1. Making Contact. *J. R. Soc., Interface* **2004**, *1*, 23−33.

(6) Ge, L.; Sethi, S.; Ci, L.; Ajayan, P. M.; Dhinojwala, A. Carbon Nanotube-Based Synthetic Gecko Tapes. *Proc. Natl. Acad. Sci. U. S. A.* **2007**, *104*, 10792−10795.

(7) Jeong, H. E.; Lee, S. H.; Kim, P.; Suh, K. Y. High Aspect-Ratio Polymer Nanostructures by Tailored Capillarity and Adhesive Force. *Colloids Surf., A* **2008**, *313−314*, 359−364.

(8) Qu, L.; Dai, L.; Stone, M.; Xia, Z.; Wang, Z. L. Carbon Nanotube Arrays with Strong Shear Binding-on and Easy Normal Lifting-Off. *Science* **2008**, *322*, 238−242.

(9) Sameoto, D.; Menon, C. Direct Molding of Dry Adhesives with Anisotropic Peel Strength Using an Offset Lift-Off Photoresist Model. *J. Micromech. Microeng.* **2009**, *19*, 115026.

(10) Tamelier, J.; Chary, S.; Turner, K. L. Vertical Anisotropic Microfibers for a Gecko-Inspired Adhesive. *Langmuir* **2012**, *28*, 8746−8752.

(11) Kim, T.-I.; Pang, C.; Suh, K. Y. Shape-Tunable Polymer Nanofibrillar Structures by Oblique Electron Beam Irradiation. *Langmuir* **2009**, *25*, 8879−8882.

(12) Greiner, C.; del Campo, A.; Arzt, E. Adhesion of Bioinspired Micropatterned Surfaces: Effects of Pillar Radius, Aspect Ratio, and Preload. *Langmuir* **2007**, *23*, 3495−3502.

(13) Bae, W.-G.; Kwak, M. K.; Jeong, H. E.; Pang, C.; Jeong, H.; Suh, K.-Y. Fabrication and Analysis of Enforced Dry Adhesives with Core.Shell Micropillars. *Soft Matter* **2013**, *9*, 1422−1427.

(14) Greiner, C.; Arzt, E.; del Campo, A. Hierarchical Gecko-Like Adhesives. *Adv. Mater.* **2009**, *21*, 479−482.

(15) Murphy, M. P.; Kim, S.; Sitti, M. Enhanced Adhesion by Gecko-Inspired Hierarchical Fibrillar Adhesives. *ACS Appl. Mater. Interfaces* **2009**, *1*, 849−855.

(16) Jeong, H. E.; Lee, J.-K.; Kim, H. N.; Moon, S. H.; Suh, K. Y. A Non Transferring Dry Adhesive with Hierarchical Polymer Nanohairs. *Proc. Natl. Acad. Sci. U. S. A.* **2009**, *106*, 5639−5644.

(17) Ho, A. Y. Y.; Yeo, L. P.; Lam, Y. C.; Rodriguez, I. Fabrication and Analysis of Gecko-Inspired Hierarchical Polymer Nanosetae. *ACS Nano* **2011**, *5*, 1897−1906.

(18) Rong, Z.; Zhou, Y.; Chen, B.; Robertson, J.; Federle, W.; Hofmann, S.; Steiner, U.; Goldberg-Oppenheimer, P. Bio-inspired

DOI: 10.1021/acsami.5b03576
ACS Appl. Mater. Interfaces 2015, 7, 16410−16417

Hierarchical Polymer Fiber−Carbon Nanotube Adhesives. *Adv. Mater.* **2014**, *26*, 1456−1461.
(19) Glass, P.; Chung, H.; Washburn, N. R.; Sitti, M. Enhanced Wet Adhesion and Shear of Elastomeric Micro-Fiber Arrays with Mushroom Tip Geometry and a Photopolymerized p (DMA-co-MEA) Tip Coating. *Langmuir* **2010**, *26*, 17357−17362.
(20) Zhou, M.; Tian, Y.; Sameoto, D.; Zhang, X.; Meng, Y.; Wen, S. Controllable Interfacial Adhesion Applied to Transfer Light and Fragile Objects by Using Gecko Inspired Mushroom-Shaped Pillar Surface. *ACS Appl. Mater. Interfaces* **2013**, *5*, 10137−10144.
(21) Li, Y.; Ahmed, A.; Sameoto, D.; Menon, C. Abigaille II: Towards the Development of a Spider-Inspired Climbing Robot. *Robotica* **2012**, *30*, 79−89.
(22) Henrey, M.; Ahmed, A.; Boscariol, P.; Shannon, L.; Menon, C. Abigaille-III: A Versatile, Bioinspired Hexapod for Scaling Smooth Vertical Surfaces. *J. Bionic Eng.* **2014**, *11*, 1−17.
(23) Lee, H.; Bhushan, B. Fabrication and Characterization of Hierarchical Nanostructured Smart Adhesion Surfaces. *J. Colloid Interface Sci.* **2012**, *372*, 231−238.
(24) Asbeck, A.; Dastoor, S.; Parness, A.; Fullerton, L.; Esparza, N.; Soto, D.; Heyneman, B.; Cutkosky, M. Climbing Rough Vertical Surfaces with Hierarchical Directional Adhesion. Presented at the IEEE International Conference on Robotics and Automation, Kobe, Japan, May 12−17, 2009.
(25) Izadi, H.; Golmakani, M.; Penlidis, A. Enhanced Adhesion and Friction by Electrostatic Interactions of Double-Level Teflon Nano-pillars. *Soft Matter* **2013**, *9*, 1985−1996.
(26) Kim, S.; Sitti, M.; Xie, T.; Xiao, X. Reversible Dry Micro-Fibrillar Adhesives with Thermally Controllable Adhesion. *Soft Matter* **2009**, *5*, 3689−3693.
(27) Roehrig, M.; Thiel, M.; Worgull, M.; Hoelscher, H. 3D Direct Laser Writing of Nano- and Microstructured Hierarchical Gecko-Mimicking Surfaces. *Small* **2012**, *8*, 3009−3015.
(28) Lee, D. Y.; Lee, D. H.; Lee, S. G.; Cho, K. Hierarchical Gecko-Inspired Nanohairs with a High Aspect Ratio Induced by Nano-yielding. *Soft Matter* **2012**, *8*, 4905−4910.
(29) Sameoto, D.; Ferguson, B. Robust Large-Area Synthetic Dry Adhesives. *J. Adhes. Sci. Technol.* **2014**, *28*, 337−353.
(30) Zhang, C.; Zhou, J.; Sameoto, D.; Zhang, X.; Li, Y.; Ng, H. W.; Menon, C.; Gates, B. D. Determining Adhesion of Nonuniform Arrays of Fibrils. *J. Adhes. Sci. Technol.* **2014**, *28*, 320−336.
(31) Li, Y.; Zhang, C.; Zhou, J. H.-W.; Menon, C.; Gates, B. D. Measuring Shear-Induced Adhesion of Gecko-Inspired Fibrillar Arrays Using Scanning Probe Techniques. *Macromol. React. Eng.* **2013**, *7*, 638−645.
(32) Li, Y.; Ng, H. W.; Gates, B. D.; Menon, C. Material Versatility Using Replica Molding for Large-Scale Fabrication of High Aspect-Ratio, High Density Arrays of Nano-pillars. *Nanotechnology* **2014**, *25*, 285303.
(33) del Campo, A.; Greiner, C.; Alvarez, I.; Arzt, E. Patterned Surfaces with Pillars with Controlled 3D Tip Geometry Mimicking Bioattachment Devices. *Adv. Mater.* **2007**, *19*, 1973−1977.
(34) Murphy, M. P.; Aksak, B.; Sitti, M. Adhesion and Anisotropic Friction Enhancements of Angled Heterogeneous Micro-Fiber Arrays with Spherical and Spatula Tips. *J. Adhes. Sci. Technol.* **2007**, *21*, 1281−1296.
(35) Joanes, D. N.; Gill, C. A. Comparing Measures of Sample Skewness and Kurtosis. *Statistician* **1998**, *47*, 183−189.
(36) Kwak, M. K.; Jeong, H. E.; Suh, K. Y. Rational Design and Enhanced Biocompatibility of a Dry Adhesive Medical Skin Patch. *Adv. Mater.* **2011**, *23*, 3949−3953.
(37) Kim, S., Spenko, M., Trujillo, S., Heyneman, B., Mattoli, V., Cutkosky, M. R. Whole Body Adhesion: Hierarchical, Directional and Distributed Control of Adhesive Forces for a Climbing Robot. Presented at the IEEE International Conference on Robotics and Automation, Roma, Italy, 10−14 April, 2007.

DOI: 10.1021/acsami.5b03576
ACS Appl. Mater. Interfaces 2015, 7, 16410−16417